

Frequency locking and travelling burst sequences in community structured network of inhibitory neurons with differing time-scales

Kunal Mozumdar^a, G. Ambika^a

^aIndian Institute of Science Education and Research, Pune, India - 411008

Abstract

We report the emergent dynamics of a community structured modular network of chaotic Hindmarsh-Rose (HR) neurons with inhibitory synapses. We find the inhibitory coupling between the neuronal modules lead to complete synchronization of neurons in a module, and also pushes modules into interesting sequences of travelling burst patterns. When dynamical time-scales vary for neurons in different modules, hence breaking the symmetry among them, we see specific sequences of travelling burst patterns that are characteristic of the time-scale mismatch and coupling strengths. Thus for a modular network with two time-scales, the neuronal communities enter into synchronized frequency locked clusters with the bursting sequences having recurring patterns. Our study provides a complete characterization of the spatio-temporal regularity in terms of frequency locking for temporal order and burst sequence patterns for spatial order in the collective dynamics of the neuronal clusters. Our results have significance in the process of information coding in terms of frequency of firing dynamics among neurons and in selective communication based on the sequences of bursts.

Keywords: Modular inhibitory neuronal networks, Multiple time-scale, Travelling bursts, Synchronized frequency locked clusters

PACS: 87.19.lj, 05.45.Xt, 82.39.Rt, 87.19.lp

1. Introduction

Studies related to the brain and its various structural and dynamical features have been a very interesting and challenging area of research in recent times. This is mainly because the brain is highly complex with over 10^9 neurons connected via complex networks perfected by evolution. Although reproducing the dynamics of the entire brain is close to impossible, due to its intricate connectome and constituent levels of its complexity, there are several generalizations in the neuronal architecture and dynamical features of the brain. These generalizations can be abstracted to give very useful mathematical models of neuronal networks, which can be extended to model the real structures in the brain. [1, 2, 3, 4]. Neuronal networks dynamically self-organize in various length and time-scales to give rise to a wide repertoire of behaviours. While the dynamical state of an individual neuron depends on the type of ion channels, their dendritic structure and the nature of coupling with other neurons, the complex behavioural aspects produced by the brain are due to the collective dynamics of several ensembles of neurons [5, 6].

In this context, community structured networks are one of the most commonly found network topology in the brain. Such networks consist of nodes that are grouped into communities based on some characteristics of the nodes or based on their connections with other nodes [7, 8]. There has been a lot of connectomics study which has pointed to the community structured or modular organization of the networks in the mammalian brain [9, 10, 11]. Some notable examples of such architecture are the striatal networks, visual cortex and olfactory lobes in insects [12] and also the layers of neurons in medial entorhinal cortex [13, 14]. Various studies have shown that this type of structure may have some role in the processing of information in neural circuits [15]. Some theoretical studies also explore the potential aspects of the modular organization leading to interesting dynamical phenomena in neuronal networks [16, 17, 18].

Several nonlinear dynamical models capture the dynamical features of individual neurons like spiking and bursts, the most widely used among them being Hindmarsh-Rose neuronal model [19] that can demonstrate a broad class of bursting dynamics [20, 21]. As is well established neurons can make contacts with other neurons through synapses

that can be excitatory or inhibitory. Specifically, several studies report the effect of inhibitory synaptic connections in neurons [22, 23, 24, 25, 26]. This type of coupling is found very crucial in producing rhythmic activity in the brain as reported by various theoretical and experimental studies [27, 28, 29, 30].

Along with the nature of connectivity among the neurons, the major factor affecting the neuronal activity is the time-scale of its dynamics. This time-scale is generally dependent on the interplay of the various ions flowing across the cell membrane of the neuron deciding its capacitance and conductance [31]. The collective activities of neurons are dependent on the temporal scales of activity of each neuron or ensemble of neurons [32, 13, 33, 34, 35] and they tend to play a major role especially in the oscillations in the midbrain region [27].

In this work, we address an important aspect of brain dynamics, viz how the presence of differing time-scales affect the emergent dynamics of the community structured neuronal networks. We start with the hypothesis that the presence of differing time-scales and inhibitory coupling can result in modulation of emergent frequencies in the system. We present a comprehensive model of a system where such variations in burst frequencies and emergence of frequency locked clusters can be studied in detail for a range of parameter values. This study in a way can model the modulation of oscillation frequencies and frequency locking reported from MEG/EEG data [36] and intra-cortical recordings [37] in primates and rats. Furthermore, such frequency locking can play a vital role in the formation of working memory.

The community structured network that we present is a very basic model that can address the dynamical complexity of the brain. It illustrates how a system of HR neurons can produce travelling burst sequences that circulate periodically among the modules. We observe a variety of dynamical states when the time-scales of the dynamics in the modules are varied. The most relevant among them are the frequency synchronized clusters with periodic sequences of bursting evident from the spatio-temporal dynamics of the network.

The model and methods of study are introduced in the next section. The results of our analysis on modular networks with identical neurons and those with time scale mismatch in their dynamics are detailed in the next three sections. The salient features and main results of the study are summarized in the final section.

2. Modular neuronal networks with differing time-scales

We start with a model of community structured network consisting of N neurons grouped into M communities or modules. The neurons in each module belong to a community since they have a specific time-scale with zero intra-connections and full inter-connections. This means they do not have any connections among themselves but each of them has inhibitory connections with the other neurons of all the other communities. For this purpose, we construct the adjacency matrix A with $(M \times M)$ block matrices B_{lk} of size $(N/M) \times (N/M)$ where $l, k = 1, 2, \dots, M$. The required community structure is established by choosing the B_{lk} s as:

$$B_{lk} = \begin{cases} [0], \forall l = k \\ [1], \forall l \neq k \end{cases} \quad (1)$$

Thus the adjacency matrix, A , in this case is given as:

$$A = \begin{bmatrix} [0] & [1] & [1] & [1] \\ [1] & [0] & [1] & [1] \\ [1] & [1] & [0] & [1] \\ [1] & [1] & [1] & [0] \end{bmatrix} \quad (2)$$

The elements of the adjacency matrix A are such that, $a_{ij} = 0$ if the neurons are in the same block ($l = k$) and $a_{ij} = 1$ if they are in different blocks ($l \neq k$). The schematic diagram in [Figure 1a](#) shows the structure thus chosen where the modules with the uncoupled neurons are represented by the colored circles. The typical values of the size of the network used in the study are $N = 120$ and $M = 4$.

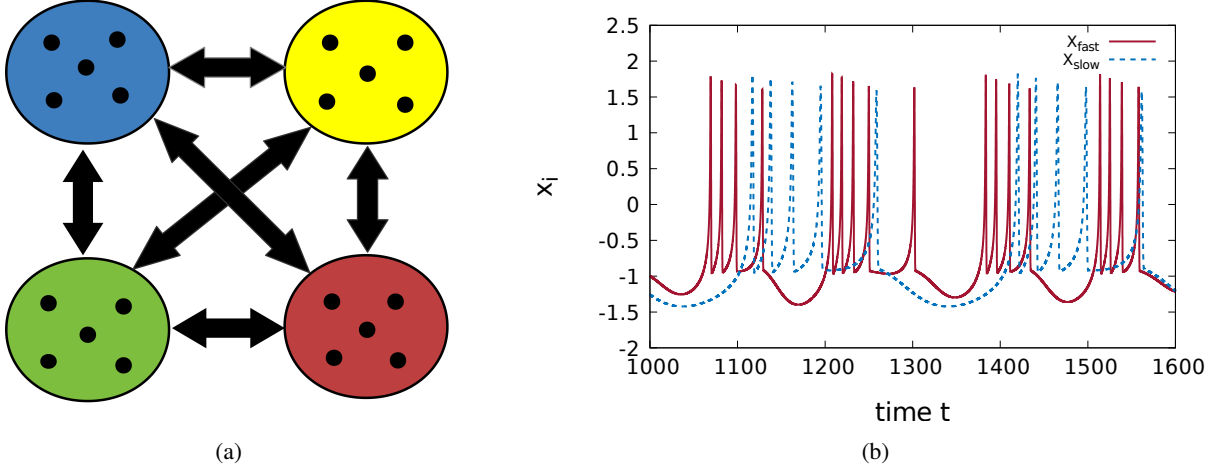


Figure 1: (Colour Online) (a) **Schematic representation of a network with modular structure:** The circles represent the modules and the dots inside each circle represent a few typical neurons. The arrows represent the all-to-all coupling between neurons of two different modules. (b) **Intrinsic dynamics of HR neuron:** The chaotic bursts for parameters $I_e = 3$ and $\epsilon = 0.006$ for a neuron (smooth line) with $(\eta = 1)$ and that for a slow neuron (dotted line) with time-scale mismatch $\eta = 0.5$

The intrinsic dynamics of each neuron is same as HR neuron and the dynamics of the i^{th} neuron as:

$$\begin{aligned}
 \dot{x}_i &= \eta_i \left(y_i - x_i^3 + 3x_i^2 - z_i + I_e - \beta(V - x_i) \sum_{j=1}^N a_{ij} \left(\frac{1}{e^{-\lambda(x_j + K)}} \right) \right) \\
 \dot{y}_i &= \eta_i (1 - 5x_i^2 - y_i) \\
 \dot{z}_i &= \eta_i (\epsilon(4(x_i + x_r) - z_i))
 \end{aligned} \tag{3}$$

Here, the variable x_i represents the membrane potential and the variable y_i and z_i represent the fast and slow gating variables of the HR neuron. We use the parameters $I_e = 3$ and $\epsilon = 0.006$ such that the intrinsic dynamics shows chaotic bursts. The synaptic coupling function is a sigmoidal function with parameters $\lambda = 10$, reversal potential $V = 2$ and synaptic threshold $K = 0.25$ respectively. This type of coupling is chosen because it is more prevalent in the brain and generates nonintuitive emergent phenomena. The nature of coupling is inhibitory and the parameter β gives the strength of coupling.

We introduce additionally a time-scale parameter determining the dynamics of each neuron as η_i , with values in the range $0 < \eta_i \leq 1$. It is clear that $\eta_i = 1$ corresponds to the regular neuronal time-scales while any values of $\eta_i < 1$ would mean the corresponding neuron being slower in dynamics than others while keeping the nature of its intrinsic dynamics the same [38]. Biologically the parameter η can be attributed to the differences in the capacitance of the axonal membranes. In Eq. 3, the parameter η can be used to tune the frequency of the neurons without affecting the dynamics of the neurons. Figure 1b shows the dynamics of two HR neurons, one of which has a slower time-scale with $\eta = 0.5$.

In this study we keep the time scale of all the neurons in each module at a specific value of the time-scale η_i . So for the whole network, time-scale parameters form a set of M values, $\boldsymbol{\eta} = (\eta_1, \eta_2, \eta_3, \eta_4)$. We initially consider a network that is symmetric both in structure and dynamics with identical neurons with all modules having the same time scale i.e. $\boldsymbol{\eta}_0 = (1, 1, 1, 1)$. In this case we analyze the emergent burst patterns of the whole network using spatio-temporal plots. Then we proceed to the more interesting case where one level of symmetry is broken by having two modules follow a slower time scale with a mismatch with the faster ones given by $\boldsymbol{\eta}_1 = (1, \eta, 1, \eta)$ (where $\eta \in [0, 1)$). We also study two other possible configurations with $\boldsymbol{\eta}_2 = (\eta, \eta, \eta, 1)$ and $\boldsymbol{\eta}_3 = (1, 1, 1, \eta)$.

In all the cases, the system of equations in Eq. 3 is analyzed by numerical simulations using fourth order vector Runge-Kutta algorithm for a step $\Delta t = 0.01$ and 600000 iterations. The first 100000 values are discarded as transients

and the remaining are used in the analysis. We present the spatio-temporal plots that provide a qualitative picture of the emergent dynamics of the network.

For a detailed characterization of the temporal dynamics, we compute the burst frequency of each neuron from its time series, x_i . We note the time τ_i^k at which the x_i values cross a threshold value of -1 with the $\dot{x} > 0$. The value of the threshold is carefully chosen after studying several cases with different parameter values for each neuron. The τ_i^k represents the time of onset of the k^{th} burst in the i^{th} neuron. The inter-burst interval (IBI) is then calculated for each burst as the time interval $\Delta\tau^k = \tau_i^{k+1} - \tau_i^k$. The average burst frequency of the i^{th} neuron is calculated using the equation:

$$f_i = \frac{2\pi}{K_i} \sum_{k=1}^{K_i} \frac{1}{\tau_i^{k+1} - \tau_i^k} \quad (4)$$

where K_i refers to the total number of bursts for the i^{th} neuron in the total time used for calculation. The intrinsic burst frequency of a single HR neuron calculated using this method turns out to be $f_o \simeq 0.04$ in arbitrary units. This generally corresponds to a frequency of ~ 60 Hz when we compare it with the biological neuronal time series [19].

3. Travelling burst dynamics

The type of topology and coupling considered in the study leads to synchronization between uncoupled neurons due to the action of inhibitory inputs from other neurons. Thus all neurons in a particular community or module are in complete synchrony with each other. In the case of two neurons, it is known that inhibitory nature of the coupling leads to anti-phase synchronization because, when one of the neurons is active it tends to inhibit the other neuron's activity. The same tendency in a modular network of mutually coupled inhibitory neurons can drive the neurons to a state of sequential bursting. So when we look at the bursting pattern in the whole network, we see each module of neurons bursts one after the other in a specific sequence like travelling bursts. The spatio-temporal plots in Figure 2 illustrate these emergent bursting patterns in the network for two different coupling strengths β .

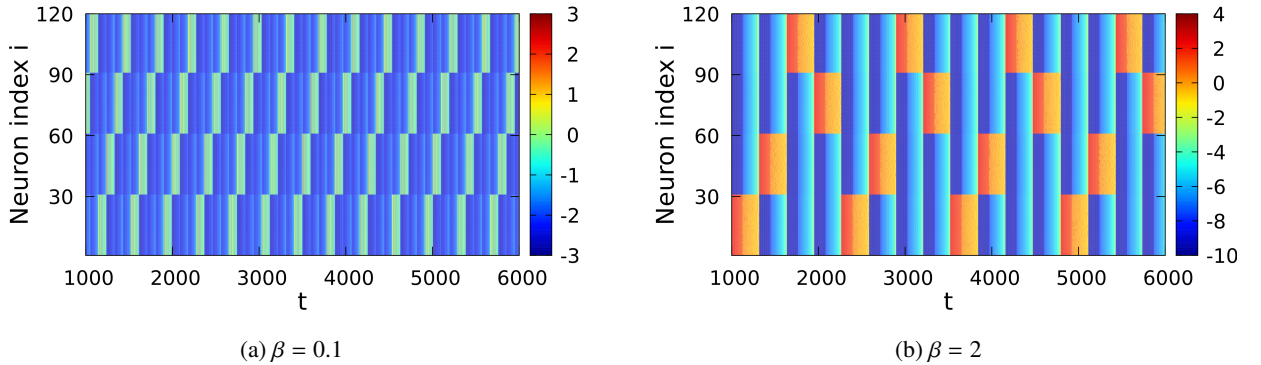


Figure 2: (Colour Online) **Spatio-temporal plots of the neuronal dynamics:**(a) $\beta = 0.1$, (b) $\beta = 2$. Each module of neurons bursts sequentially one after the other in time, producing a travelling burst pattern in the network.

We can infer a few general trends in the dynamics of the network from the spatio-temporal plots in Figure 2. Firstly, the bursting sequence remains periodic as the whole system evolves in time. This means the inhibitory coupling drives the system of chaotic bursting neurons into periodic square bursting dynamics. Secondly, the bursting dynamics is identical in all the modules, i.e., all the neurons show identical mixed-mode square bursting dynamics, although the bursts are shifted in space and time. This is illustrated in Figure 3 where the time series of typical neurons from each module corresponding to the states of spatio-temporal plots in Figure 2 are shown.

We calculate the burst frequency of each neuron averaged over the module, using Eq. 4. This remains the same for all the modules for a given β , indicating frequency synchronization over the whole network, even though the bursts

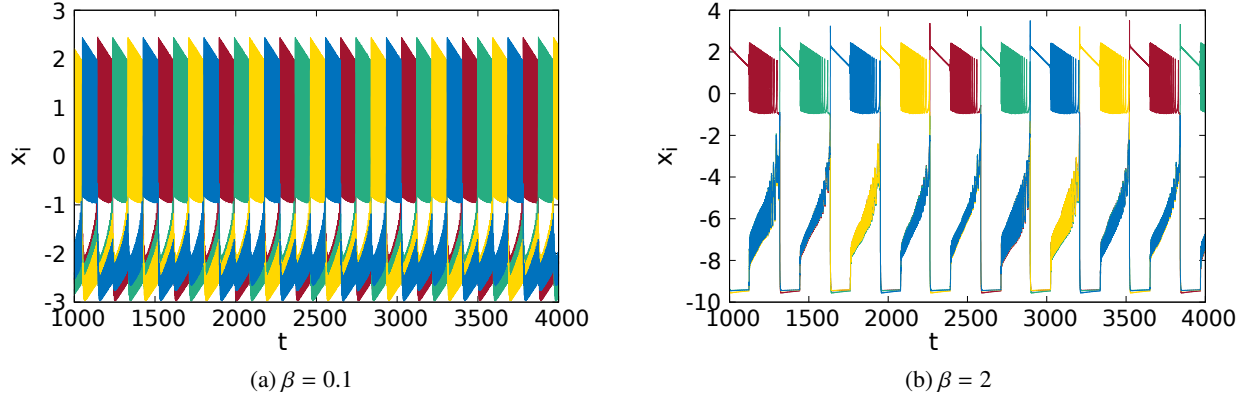


Figure 3: (Colour Online) **Time series of sequentially bursting neurons from each module:**(a) $\beta = 0.1$, (b) $\beta = 2$. The dynamics of typical neurons from each module (for $i = 30, 60, 90, 120$) is shown. It is clear that all neurons have the same periodic bursts that form a sequential pattern of bursting. With increase in β , the time period of the burst increases.

are shifted in phase. Moreover, as is clear from the Figure 3, the bursting frequency decreases as β increases. In the context of neurons, the synaptic coupling strength β can vary according to certain plasticity rules [39]. Our results indicate how this variation in β can modulate the frequency of the collective dynamics of neurons. This is shown in Figure 4 where $f_{av} \approx \beta^{-\nu}$. We note that frequency of the whole network is less than the intrinsic frequency of the neurons. For the case of the symmetric network discussed so far, with identical neurons, with $\eta_0 = (1, 1, 1, 1)$, all the neurons are frequency synchronized and the firing pattern has a wave of travelling bursts circulating over the whole network periodically.

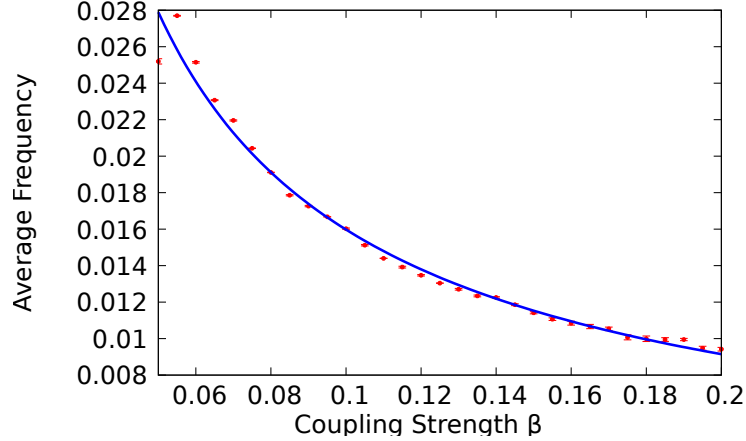


Figure 4: (Colour Online) **Frequency vs Coupling Strength:** The dotted circles indicate the calculated frequency averaged over the network for five realizations. The smooth line shows the function fit to the mean values, $f_{av} = A\beta^{-\nu}$ where the values are given as $A = 0.0025 \pm 0.0001$ and $\nu = 0.80 \pm 0.02$.

4. Bursts sequences with differing time-scales

In this section, we present the study on the modular network with a time-scale parameter is not the same in all the modules. The differing time-scales break the symmetry of the network, as now the neurons in one module are non-identical with that in another. As a specific case we consider, two slow communities and two fast ones with the time-scales fixed as $\eta_1 = (1, \eta, 1, \eta)$.

Our numerical analysis shows that in this case also, the travelling burst pattern occurs with the neurons in each module bursting sequentially one after the other. But the pattern of bursting is decided by the value of the time-scale η . This is evident from the spatio-temporal dynamics on the network as shown in Figure 5, for three different values of η . We label each particular sequence by P_k^η . For example, for $\eta = 0.9$, we identify the sequence of the travelling bursts from Figure 5a as $P_1^\eta = \overline{S_1 S_2 F_1 F_2}$, where S_1, S_2 and F_1, F_2 represent the slow and fast community, numbered according to the order in which communities burst in time. The bar over the sequence indicates that the sequence is repeated periodically in time.

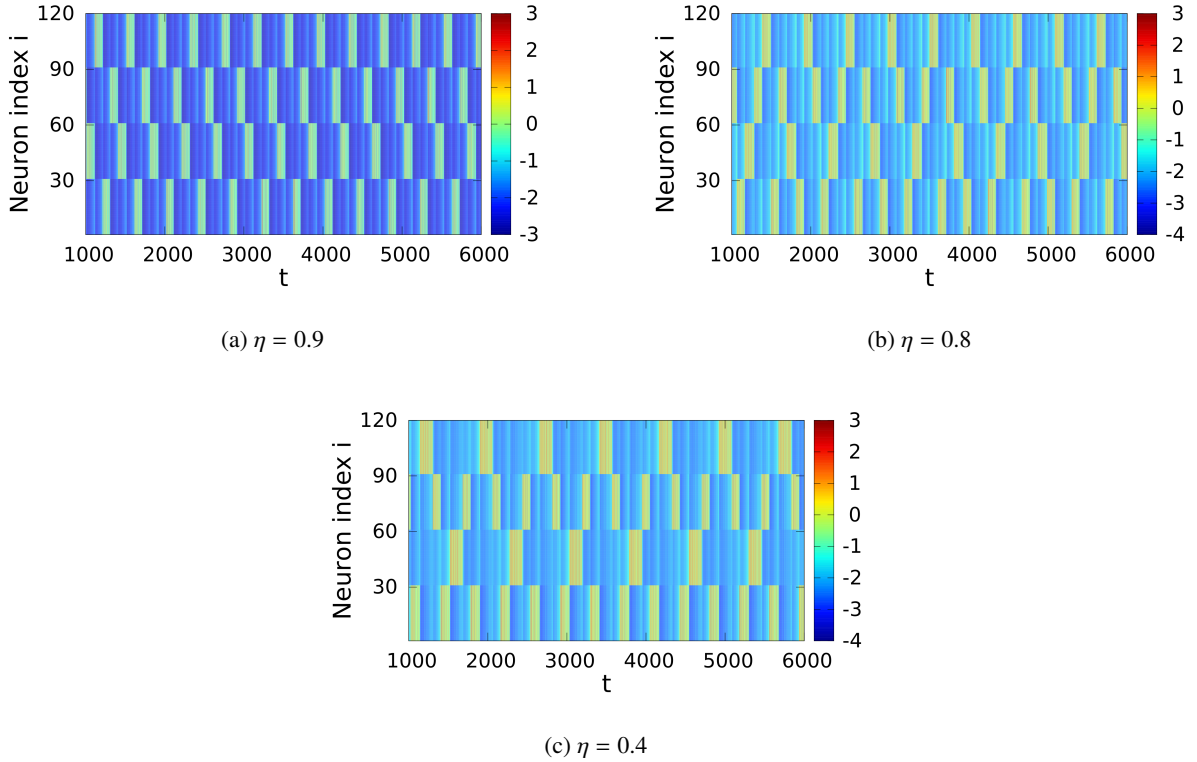


Figure 5: (Colour Online) **Spatio-temporal plots of the neuronal dynamics with time-scale mismatch at $\beta = 0.1$:** (a) $\eta = 0.9$, showing the sequence P_1^η . (b) $\eta = 0.8$, P_2^η . (c) $\eta = 0.4$, P_3^η .

As η is lowered to a value of $\eta = 0.8$, the travelling bursts have a longer sequence $P_2^\eta = \overline{F_1 S_1 F_2 S_2 F_1 F_2 S_1 F_1 S_2 F_2}$ with slow communities bursting four times and fast communities bursting six times during the time of one cycle, as shown in Figure 5b. At lower values of η , like in Figure 5c, ($\eta = 0.4$) the bursting pattern changes to $P_3^\eta = \overline{S_2 F_2 F_1 S_1 F_2 F_1}$ so that the slower modules burst once each and the faster modules burst twice in one cycle. In all cases, the sequences are repeated periodically in time. We prescribe a characterization of the periodic bursting sequences as $(p : q)$ where p represent the number of slow bursts and q represent the number of fast bursts. Then, with time scales fixed as $\eta_1 = (1, \eta, 1, \eta)$, the network has 3 different emergent dynamical states of the network, that can be denoted by $(2 : 2)$, $(4 : 6)$ and $(2 : 4)$ for decreasing values of η .

We now present two more possible configurations of the network that are more heterogeneous with unequal number of slow and fast modules, with 3 slow and 1 fast modules ($\eta_2 = (\eta, \eta, \eta, 1)$), and with 1 slow and 3 fast modules ($\eta_3 = (1, 1, 1, \eta)$). In a network of four modules, these exhaust all possible configurations. We have summarized these results in Table 1 and Figure 6 highlighting the ranges of η values for each burst sequence for all the three cases in the present study. By extending the study along similar lines to networks with larger number of modules, we expect a variety of interesting periodic patterns of bursting based on the numbers of slow and fast modules and the distribution of η values among them.

Burst sequences in four modules			
Configuration (η_i)	Sequence ($P_j^{\eta_i}$)	($p : q$)	Range of η
$\eta_1 = (1, \eta, 1, \eta)$	$P_1^{\eta_1} = \overline{S_3 S_2 S_1 F}$	(3 : 1)	[0.83, 1]
	$P_2^{\eta_1} = \overline{F_1 S_1 F_2 S_2 F_1 F_2 S_1 F_1 S_2 F_2}$	(4 : 6)	(0.76, 0.82]
	$P_3^{\eta_1} = \overline{S_2 F_2 F_1 S_1 F_2 F_1}$	(2 : 4)	[0.4, 0.76]
$\eta_2 = (\eta, \eta, \eta, 1)$	$P_1^{\eta_2} = \overline{F S_3 F S_2 F S_1}$	(3 : 3)	[0.83, 1]
	$P_2^{\eta_2} = \overline{F S_3 S_2 F S_1 S_3 F S_2 S_1 F}$	(6 : 4)	[0.6, 0.83)
	$P_3^{\eta_2} = \overline{S_3 F S_2 S_1 F}$	(3 : 2)	[0.54, 0.6)
	$P_4^{\eta_2} = \overline{F S_3 F S_2 F S_1}$	(3 : 3)	[0.3, 0.54)
$\eta_3 = (1, 1, 1, \eta)$	$P_1^{\eta_3} = \overline{F_3 F_2 F_1 S}$	(1 : 3)	(0.78, 1]
	$P_2^{\eta_3} = \overline{S F_3 F_1 F_2 F_3 S F_1 F_2 F_3 F_1 S F_2 F_3 F_1 F_2}$	(3 : 12)	(0.72, 0.78]
	$P_3^{\eta_3} = \overline{S F_1 F_3 F_2 F_1 F_3 S F_2 F_1 F_3 F_3 F_1 S F_3 F_2 F_1 F_3 F_2}$	(3 : 15)	(0.66, 0.72]
	$P_4^{\eta_3} = \overline{S F_3 F_2 F_1 F_3 F_2 F_1 F_3 F_2 F_1}$	(1 : 9)	(0.63, 0.66]
	$P_5^{\eta_3} = \overline{F_3 F_2 F_1}$	(0 : 3)	[0.3, 0.63]

Table 1: Burst patterns and their sequences for the three configurations with four modules for $\beta = 0.1$. The range of time-scale values for which they are stable are also given in the rightmost column.

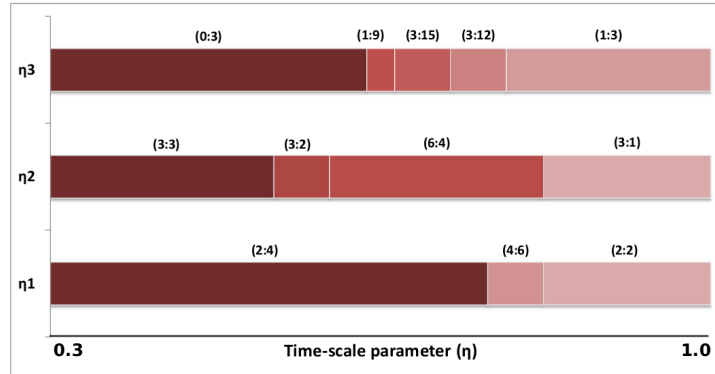


Figure 6: (Colour Online) Schematic representation of the burst sequences observed in the three configurations of the modules for $\beta = 0.1$: For each configuration, the different sequences are in different colours with ($p : q$) values given above.

5. Frequency locked clusters

The pattern of sequences reported in Section 4 can be further quantified by calculating the average burst frequency for each community of neurons as $\mathbf{f} = (f_1, f_2, f_3, f_4)$ using Eq. 4. For the case of two slow and two fast modules, the frequencies for different η values with $\beta = 0.1$ for each module is shown in Figure 7a. It is clear that for sufficiently small mismatch or large η , all the modules in the network are still in a single frequency synchronized state with the average frequency much less than the intrinsic value. As η is reduced, we find the single frequency state bifurcates into a state where the two slow and the two fast modules separate into two different clusters of differing frequencies, while being synchronized among them.

We find that the bursts in the slow and fast modules are locked into specific ratios. This ratio ρ , of the average frequency of neurons in the slow modules and that of neurons in the fast modules, can thus characterize the locked

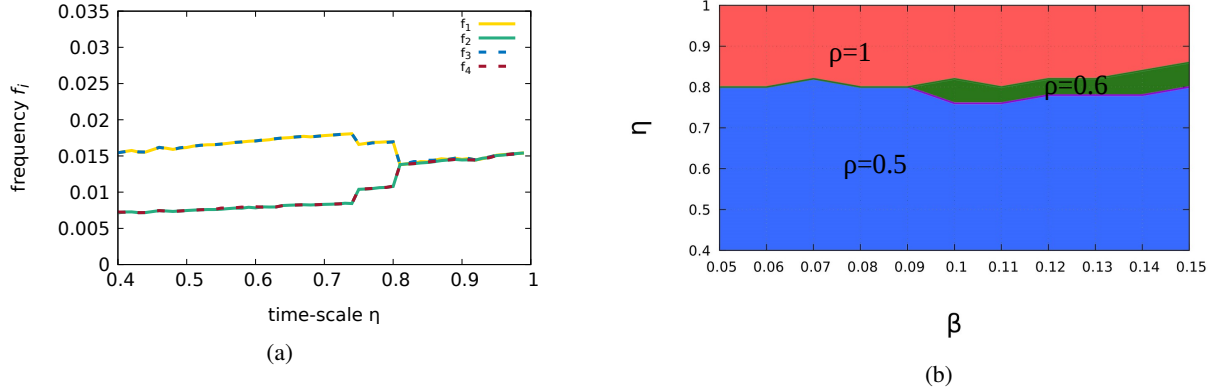


Figure 7: (Colour Online) **(a) Frequency vs time-scale parameter at $\beta = 0.1$ for configuration η_1 :** For large η or less mismatch in time-scale the whole network is synchronized at a single frequency. At lower values of η , there are two distinct clusters of slow and fast frequencies. **(b) Regions in the (β, η) parameter space for configuration η_1 :** The three regions correspond to the three distinct synchronized frequency locked states - Red(gray) region corresponds to the state $\rho = 1$, green(black) region to $\rho = 0.6$ and blue(dark gray) region to $\rho = 0.5$.

states. For the network with two slow and two fast modules, we get three distinct ratios, 1, 0.5 and 0.6. The values of the parameters for which the locked states stabilize, are indicated in the parameter plane (β, η) in Figure 7b. It is interesting to note that while the frequency values of each cluster keep changing with β and η , the locking ratio remains constant over a sufficient region of the plane.

These frequency locked states correspond directly to the three patterns of spatial burst sequences mentioned above and seen in the spatio-temporal plots in Figure 5. Thus $\rho = 1$ corresponds to the state $(2 : 2)$, $\rho = \frac{1}{2}$ corresponds to state $(2 : 4)$, and $\rho = \frac{2}{3}$ corresponds to the state $(4 : 6)$. Thus the frequency ratio and the burst sequences together characterize the spatio-temporal dynamics of the neurons fully.

6. Discussions

In this study we report the emergent dynamics and bursting patterns produced in a modular network of neurons with inhibitory couplings. The modules in the network are organized based on the type of coupling and the dynamical time-scales. Primarily our study emphasizes the role of inhibitory couplings in inducing regulated patterns of synchrony among neurons which are not coupled directly to each other. It also indicates how the frequency of the whole network gets modified due to variations in the synaptic coupling strength.

We show that a variety of dynamical states are possible when the time-scales of the dynamics in the communities are different. The travelling burst dynamics observed in this case is specific to the mismatch in time-scales and can be uniquely characterized by the frequency ratios. The slow and fast time-scales in each module result in specific emergent frequencies in it, which in the presence of inhibitory couplings among them, drive the whole network to fire at various patterns of bursting sequences. The resultant spatio-temporal regularity in the collective dynamics is fully characterized by analyzing the sequential order in the burst patterns and the frequency locking in temporal order. By changing the time-scale mismatch parameter, we observe frequency synchronized clusters that are locked into ratios like 1, $\frac{1}{2}$ and $\frac{2}{3}$, etc. and are stable over a finite region of the parameter plane of time-scale and coupling strength.

As is well known, the frequency of bursting or firing in the dynamics of connected neurons has a major role in the coding and transmission of information among them [40, 41, 42] especially in selective communication [43]. Also, frequency locking and modulation are associated with integrating sensory information to form working memory and retrieval of such memory for sensory-guided tasks [44, 45]. In response to input currents, synaptic strengths, and heterogeneous synapses, modulation in frequency and frequency locked states have been reported earlier [46, 47, 48]. But frequency locking and bursting sequences combining temporal and spatial dynamics due to heterogeneous time-scales is a novel phenomenon reported in this work.

By extending the model to a larger number of modules and varying the time scale mismatches among them, a variety of sequences can be generated. These bursting sequences themselves can thus be a mechanism or medium for

coding information.

7. References

References

- [1] E. Bullmore, O. Sporns, Complex brain networks: graph theoretical analysis of structural and functional systems., *Nature Reviews Neuroscience* 10 (3).
- [2] E. M. Izhikevich, *Dynamical systems in neuroscience*, MIT press, 2007.
- [3] P. Ashwin, S. Coombes, R. Nicks, Mathematical frameworks for oscillatory network dynamics in neuroscience, *The Journal of Mathematical Neuroscience* 6 (1) (2016) 2.
- [4] D. Parker, V. Srivastava, Dynamic systems approaches and levels of analysis in the nervous system, *Frontiers in Physiology* 4.
- [5] T. Womelsdorf, J.-M. Schoffelen, R. Oostenveld, W. Singer, R. Desimone, A. K. Engel, P. Fries, Modulation of neuronal interactions through neuronal synchronization, *Science* 316 (5831) (2007) 1609–1612.
- [6] I. Belykh, M. Hasler, Mesoscale and clusters of synchrony in networks of bursting neurons, *Chaos: An Interdisciplinary Journal of Nonlinear Science* 21 (1) (2011) 016106.
- [7] M. E. Newman, Modularity and community structure in networks, *Proceedings of the National Academy of Sciences* 103 (23) (2006) 8577–8582.
- [8] J. Stroud, M. Barahona, T. Pereira, Dynamics of cluster synchronisation in modular networks: Implications for structural and functional networks, in: *Applications of Chaos and Nonlinear Dynamics in Science and Engineering-Vol. 4*, Springer, 2015, pp. 107–130.
- [9] D. Meunier, R. Lambiotte, E. T. Bullmore, Modular and hierarchically modular organization of brain networks, *Frontiers in Neuroscience* 4.
- [10] P. M. Gleiser, V. I. Spoomaker, Modelling hierarchical structure in functional brain networks, *Philosophical Transactions of the Royal Society of London A: Mathematical, Physical and Engineering Sciences* 368 (1933) (2010) 5633–5644.
- [11] C. Nicolini, A. Bifone, Modular structure of brain functional networks: breaking the resolution limit by surprise, *Scientific Reports* 6.
- [12] C. Assisi, M. Stopfer, M. Bazhenov, Using the structure of inhibitory networks to unravel mechanisms of spatiotemporal patterning, *Neuron* 69 (2) (2011) 373–386.
- [13] C. J. Honey, R. Kötter, M. Breakspear, O. Sporns, Network structure of cerebral cortex shapes functional connectivity on multiple time scales, *Proceedings of the National Academy of Sciences* 104 (24) (2007) 10240–10245.
- [14] D. Angulo-Garcia, J. D. Berke, A. Torcini, Cell assembly dynamics of sparsely-connected inhibitory networks: a simple model for the collective activity of striatal projection neurons, *PLoS Computational Biology* 12 (2).
- [15] A. Kumar, S. Rotter, A. Aertsen, Spiking activity propagation in neuronal networks: reconciling different perspectives on neural coding, *Nature reviews. Neuroscience* 11 (9) (2010) 615.
- [16] X. Yang, H. Li, Z. Sun, Partial coupling delay induced multiple spatiotemporal orders in a modular neuronal network, *PloS one* 12 (6) (2017) e0177918.
- [17] J. Hizanidis, N. E. Kouvaris, Z.-L. Gorka, A. Díaz-Guilera, C. G. Antonopoulos, Chimera-like states in modular neural networks, *Scientific Reports* 6.
- [18] M. Santos, J. Szezech, F. Borges, K. Iarosz, I. Caldas, A. Batista, R. Viana, J. Kurths, Chimera-like states in a neuronal network model of the cat brain, *Chaos, Solitons & Fractals* 101 (2017) 86–91.
- [19] J. L. Hindmarsh, R. Rose, A model of neuronal bursting using three coupled first order differential equations, *Proceedings of the Royal Society of London B: Biological Sciences* 221 (1222) (1984) 87–102.
- [20] R. Barrio, M. Angeles Martínez, S. Serrano, A. Shilnikov, Macro-and micro-chaotic structures in the hindmarsh-rose model of bursting neurons, *Chaos: An Interdisciplinary Journal of Nonlinear Science* 24 (2) (2014) 023128.
- [21] G. Innocenti, A. Morelli, R. Genesio, A. Torcini, Dynamical phases of the hindmarsh-rose neuronal model: Studies of the transition from bursting to spiking chaos, *Chaos: An Interdisciplinary Journal of Nonlinear Science* 17 (4) (2007) 043128.
- [22] C. Van Vreeswijk, L. Abbott, G. B. Ermentrout, When inhibition not excitation synchronizes neural firing, *Journal of Computational Neuroscience* 1 (4) (1994) 313–321.
- [23] T. J. Lewis, J. Rinzel, Dynamics of spiking neurons connected by both inhibitory and electrical coupling, *Journal of Computational Neuroscience* 14 (3) (2003) 283–309.
- [24] C. Assisi, M. Bazhenov, Synaptic inhibition controls transient oscillatory synchronization in a model of the insect olfactory system, *Frontiers in Neuroengineering* 5.
- [25] C. Börgers, N. Kopell, Synchronization in networks of excitatory and inhibitory neurons with sparse, random connectivity, *Neural computation* 15 (3) (2003) 509–538.
- [26] E. Catsigeras, Chaos and stability in a model of inhibitory neuronal network, *International Journal of Bifurcation and Chaos* 20 (02) (2010) 349–360.
- [27] G. Buzsáki, A. Draguhn, Neuronal oscillations in cortical networks, *science* 304 (5679) (2004) 1926–1929.
- [28] X.-J. Wang, G. Buzsáki, Gamma oscillation by synaptic inhibition in a hippocampal interneuronal network model, *Journal of Neuroscience* 16 (20) (1996) 6402–6413.
- [29] V. S. Sohal, J. R. Huguenard, Inhibitory coupling specifically generates emergent gamma oscillations in diverse cell types, *Proceedings of the National Academy of Sciences* 102 (51) (2005) 18638–18643.
- [30] J. A. White, M. I. Banks, R. A. Pearce, N. J. Kopell, Networks of interneurons with fast and slow γ -aminobutyric acid type a (gaba) kinetics provide substrate for mixed gamma-theta rhythm, *Proceedings of the National Academy of Sciences* 97 (14) (2000) 8128–8133.
- [31] R. Echeveste, C. Gros, Drifting states and synchronization induced chaos in autonomous networks of excitable neurons, *Frontiers in Computational Neuroscience* 10.

- [32] J. Rubin, M. Wechselberger, The selection of mixed-mode oscillations in a hodgkin-huxley model with multiple timescales, *Chaos: An Interdisciplinary Journal of Nonlinear Science* 18 (1) (2008) 015105.
- [33] T. Kispersky, J. A. White, H. G. Rotstein, The mechanism of abrupt transition between theta and hyper-excitable spiking activity in medial entorhinal cortex layer ii stellate cells, *PloS one* 5 (11) (2010) e13697.
- [34] Y. Yamashita, J. Tani, Emergence of functional hierarchy in a multiple timescale neural network model: a humanoid robot experiment, *PLoS Computational Biology* 4 (11) (2008) e1000220.
- [35] D. Papo, Time scales in cognitive neuroscience, *Frontiers in Physiology* 4.
- [36] F. Siebenhühner, S. H. Wang, J. M. Palva, S. Palva, Cross-frequency synchronization connects networks of fast and slow oscillations during visual working memory maintenance, *Elife* 5 (2016) e13451.
- [37] Y. Penn, M. Segal, E. Moses, Network synchronization in hippocampal neurons, *Proceedings of the National Academy of Sciences* 113 (12) (2016) 3341–3346.
- [38] K. Gupta, G. Ambika, Suppression of dynamics and frequency synchronization in coupled slow and fast dynamical systems, *The European Physical Journal B* 89 (6) (2016) 147.
- [39] L. F. Abbott, S. B. Nelson, Synaptic plasticity: taming the beast, *Nature Neuroscience* 3 (11s) (2000) 1178.
- [40] A. Borst, F. E. Theunissen, Information theory and neural coding, *Nature Neuroscience* 2 (11) (1999) 947–957.
- [41] B. B. Averbeck, D. Lee, Coding and transmission of information by neural ensembles, *Trends in Neurosciences* 27 (4) (2004) 225–230.
- [42] R. B. Stein, The information capacity of nerve cells using a frequency code, *Biophysical Journal* 7 (6) (1967) 797–826.
- [43] E. M. Izhikevich, N. S. Desai, E. C. Walcott, F. C. Hoppensteadt, Bursts as a unit of neural information: selective communication via resonance, *Trends in Neurosciences* 26 (3) (2003) 161–167.
- [44] P. Tiesinga, T. J. Sejnowski, Cortical enlightenment: are attentional gamma oscillations driven by ing or ping?, *Neuron* 63 (6) (2009) 727–732.
- [45] T. Womelsdorf, P. Fries, The role of neuronal synchronization in selective attention, *Current opinion in neurobiology* 17 (2) (2007) 154–160.
- [46] R. Stoop, J. Buchli, M. Christen, Phase and frequency locking in detailed neuron models, in: *Proceedings of the international symposium on nonlinear theory and its applications (NOLTA)*, 2004, pp. 43–6.
- [47] E. Lowet, M. Roberts, A. Hadjipapas, A. Peter, J. van der Eerden, P. De Weerd, Input-dependent frequency modulation of cortical gamma oscillations shapes spatial synchronization and enables phase coding, *PLoS Computational Biology* 11 (2) (2015) e1004072.
- [48] C. C. Chow, J. A. White, J. Ritt, N. Kopell, Frequency control in synchronized networks of inhibitory neurons, *Journal of Computational Neuroscience* 5 (4) (1998) 407–420.